

Annual Review of Food Science and Technology
Mechano-Bactericidal Surfaces:
Mechanisms, Nanofabrication,
and Prospects for Food
Applications

Yifan Cheng,^{1,3} Xiaojing Ma,¹ Trevor Franklin,¹
Rong Yang,¹ and Carmen I. Moraru²

¹Robert F. Smith School of Chemical and Biomolecular Engineering, Cornell University, Ithaca, New York, USA; email: ryang@cornell.edu

²Department of Food Science, Cornell University, Ithaca, New York, USA;
email: cim24@cornell.edu

³Department of Food Science and Technology, Virginia Tech, Blacksburg, Virginia, USA;
email: yifancheng@vt.edu

ANNUAL
REVIEWS **CONNECT**

www.annualreviews.org

- Download figures
- Navigate cited references
- Keyword search
- Explore related articles
- Share via email or social media

Annu. Rev. Food Sci. Technol. 2023. 14:449–72

The *Annual Review of Food Science and Technology* is online at food.annualreviews.org

<https://doi.org/10.1146/annurev-food-060721-022330>

Copyright © 2023 by the author(s). This work is licensed under a Creative Commons Attribution 4.0 International License, which permits unrestricted use, distribution, and reproduction in any medium, provided the original author and source are credited. See credit lines of images or other third-party material in this article for license information.



Keywords

mechano-bactericidal surfaces, nanofabrication, food-contact surfaces, food processing, food packaging, antimicrobial

Abstract

Mechano-bactericidal (MB) nanopatterns have the ability to inactivate bacterial cells by rupturing cellular envelopes. Such biocide-free, physico-mechanical mechanisms may confer lasting biofilm mitigation capability to various materials encountered in food processing, packaging, and food preparation environments. In this review, we first discuss recent progress on elucidating MB mechanisms, unraveling property–activity relationships, and developing cost-effective and scalable nanofabrication technologies. Next, we evaluate the potential challenges that MB surfaces may face in food-related applications and provide our perspective on the critical research needs and opportunities to facilitate their adoption in the food industry.

1. BIOFILM REDUCTION WITH MATERIAL-CENTRIC STRATEGIES

Microbial contamination of material surfaces throughout the food supply chain is a leading cause of foodborne illness and food loss. Globally, bacterial pathogens were estimated to be responsible for 60% of foodborne illnesses and 65% of deaths (estimated ~187,000) (DeFlorio et al. 2021, Havelaar et al. 2015). Additionally, it has been estimated that spoilage due to microbial contamination, along with product expiration, causes annual food losses amounting to 33%–50% of global food production (Machell et al. 2015). One major route of microbial contamination is through the transfer of persistent microorganisms from various surfaces within the food-handling environments (e.g., processing, packaging, storage, or preparation) to food products (Cools et al. 2005, Vorst et al. 2006). These surface-associated microbes often exist in biofilms, which are communities of microorganisms (of single or multiple species) bound together by extracellular polymeric substances (EPSs). Microbes in biofilms are more resistant to various sanitation methods used in the food industry than their planktonic counterparts (Frank & Koffi 1990). In food processing and handling environments, biofilms can inhabit surfaces of a wide variety of materials, including stainless steel (SS), plastics, rubber, and cellulosic materials. They can also thrive within a multitude of environments, including at solid–liquid (e.g., inner pipe walls immersed in milk or beverages) or solid–liquid–gas (e.g., conveyer belt surfaces partially wetted by meat or poultry cuts) interfaces. The versatility of biofilms, in combination with their resistance to antimicrobial measures, make them a persistent threat to food safety and quality and lead to dire economic and health consequences (Mattila-Sandholm & Wirtanen 1992). To disrupt and remove bacterial biofilms in food-handling environments, physical (hot steam, ultrasonication, etc.), chemical (solutions of sodium hypochlorite, quaternary ammonium compounds, peracetic acid, etc.), and biological (bacteriophage, enzymes, bacteriocins) treatments, or their combinations, are often implemented (Galié et al. 2018). Although effective in many cases, these treatments rely on proper and repeated application to achieve and maintain the intended reduction of microbial load. Additionally, favorable growth conditions of bacteria in the food processing environment and their adaptation to sublethal levels of chemical sanitizers could, if neglected, result in less bactericidal efficacy of the sanitizing methods than was obtained in validation studies (Harrand et al. 2019, 2021).

Material-centric antibacterial solutions, enabled by surface engineering of solid materials, have garnered much research interest lately, as they have shown promise in reducing biofilm formation via various antifouling or killing mechanisms. Material-centric solutions often focus on interfering with the early stages of the biofilm life cycle (Toole et al. 2000), slowing down or even halting the progression to mature, persistent biofilms (Cheng et al. 2019, Franklin & Yang 2020). Advances in nanofabrication and nanoengineering facilitated the development of nanopatterned surfaces with surface topographies reminiscent of those found in nature that fend off microbial invasion via physical perturbation instead of (bio)chemical effects (Linklater et al. 2020). Despite the antimicrobial potential of these mechano-bactericidal (MB) surfaces, their implementation in the food industry as a solution for improving food safety and quality is hindered by a unique set of challenges, including scalability, cost-effectiveness, mechanical and chemical durability, and complex food matrix composition (Bastarrachea et al. 2015).

In this review, we aim to critically discuss MB research advances and solutions with potential for food applications and highlight the need for future translational research that could speed up their practical applications and thus benefit food safety and quality.

2. MECHANO-BACTERICIDAL NANOTOPOGRAPHIES AND MECHANISMS OF ACTION

2.1. Surfaces that Induce Physicomechanical Inactivation of Microorganisms

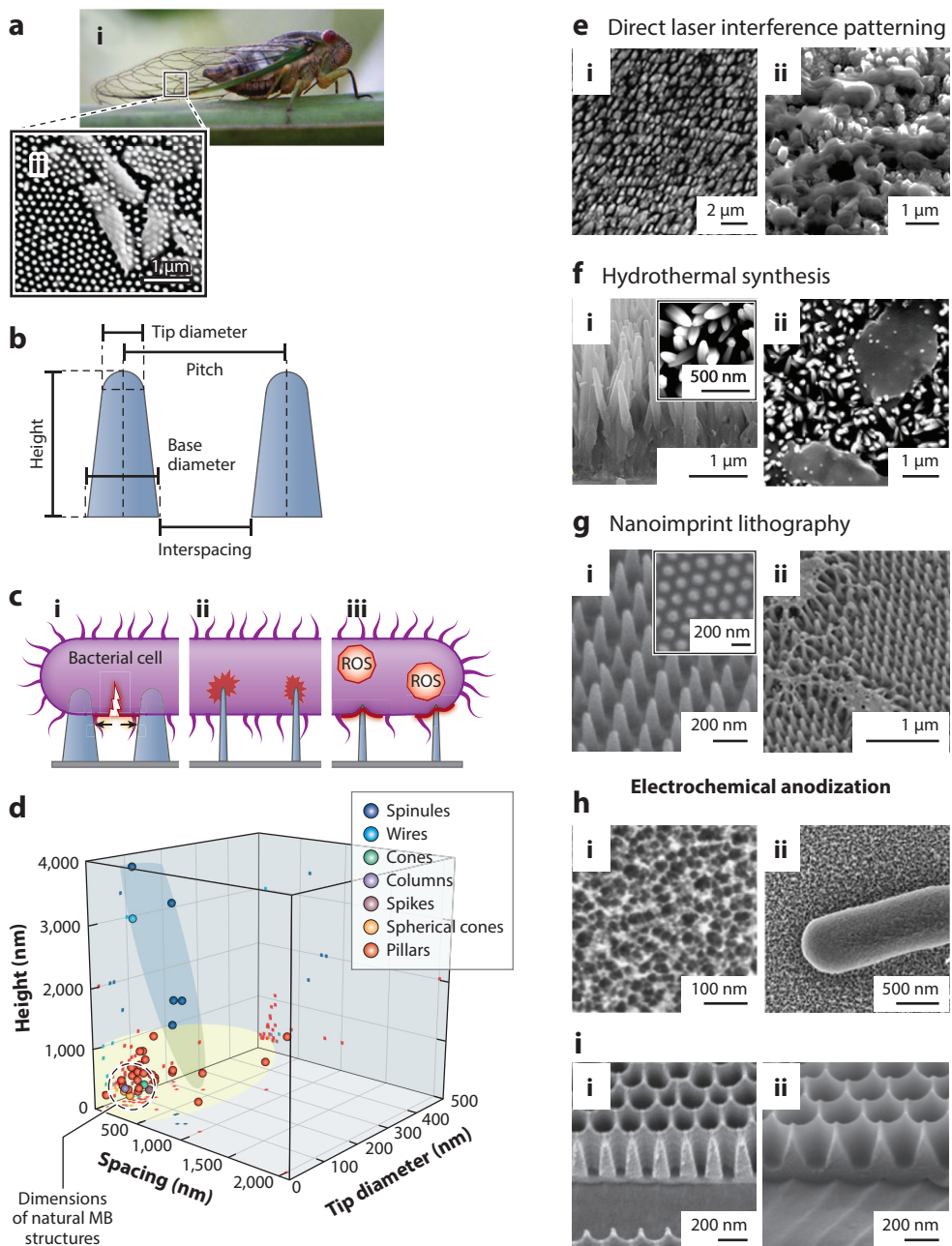
Nature has devised ingenious MB surface designs that provided inspiration for synthetic analogs on a wide range of human-made materials. A deep understanding of the MB mechanisms and property–activity relationships through both experiments and models, either analytical or numerical, can lead to guiding principles that will enable improved MB efficacy. The availability of affordable and scalable nanofabrication technologies is equally important, as these are the key to materializing the design principles to produce surfaces with practical applications in the food industry and related areas.

2.1.1. Natural and biomimetic mechano-bactericidal surfaces. Since the discovery of the MB phenomenon of the nanopillared surfaces on cicada wings (**Figure 1a**) (Ivanova et al. 2012), various naturally evolved nanopattern designs have been reported to possess extraordinary bactericidal activity. Such natural MB nanopatterns are found on the wings of several species of cicadas and dragonflies (Bandara et al. 2017; Ivanova et al. 2012, 2013), on the surface of moth eyes (Minoura et al. 2017), and on the skin of gecko lizards (Watson et al. 2015). These natural MB nanopatterns typically consist of nanoscale protrusions with a diameter of ~50–250 nm and are present on critical surfaces (e.g., wings) where the need to minimize biofilm accumulation intersects with the challenge of effective cleaning or sanitization (Tripathy et al. 2017). This is reminiscent of the situation encountered within food processing environments, where thorough cleaning and sanitization require disassembling of parts or even the entire processing equipment, causing unwelcomed downtime and significant labor costs. Thus, replicating such natural nanopatterns on food-contact surfaces represents an attractive approach to mitigate contamination, improve productivity, and reduce operating costs. Although the exact mechanisms by which cicada and the other aforementioned organisms synthesize nanopatterns from biomolecular building blocks remain unclear, recent advances in surface nanoengineering offered ways to generate nanostructures that mimic these natural MB nanopatterns on materials such as silicon, glass, metal/metal oxides, and polymers (Jaggesar et al. 2017). Some of the nanoengineered synthetic alternatives also enable tuning of variable topographical parameters to improve on the mechanisms underpinning the naturally occurring patterns, as discussed in Sections 2.1.3 and 2.1.4.

2.1.2. Mechano-bactericidal efficacy affected by the bacterial cell wall structure. The efficacy of MB inactivation depends strongly on the architecture of the bacterial cell walls because the physicomechanical disruption of the cell envelope is the primary killing mechanism (see Section 2.1.3). In general, from the outmost layer inward, the cell envelope of a Gram-negative bacterium (e.g., *Pseudomonas aeruginosa*, *Escherichia coli*) is composed of an outer membrane with lipopolysaccharides extending from its surface (~40 nm), a thin peptidoglycan layer (7–8 nm) situated in the periplasmic space, and an inner membrane, also known as the plasma or cytoplasmic membrane (~6 nm). In keeping with conventions, in this review, the “cell wall” of a bacterium refers only to the portion of the cell envelope beyond the cytoplasmic membrane (Beveridge 1999). In contrast, a Gram-positive bacterium (e.g., *Staphylococcus aureus*, *Bacillus subtilis*) envelope features a thicker (30–100 nm) peptidoglycan layer, with embedded teichoic acids and lipoteichoic acids, and an underlying cytoplasmic membrane (~6 nm) (De Geyter et al. 2016, Tripathy et al. 2017). Gram-positive bacteria, owing to their thicker cell wall (mainly peptidoglycan) and greater stretching modulus, exhibit higher tolerance to physicomechanical disruption inflicted by a wide range of MB nanostructures of either natural or synthetic origins compared to Gram-negative bacteria (Ganjian et al. 2019, Hasan et al. 2013, Ivanova et al. 2020, Linklater et al. 2022,

Wandiyanto et al. 2020). This has important implications for designing and deploying MB surfaces for food applications, given the prevalence of either Gram-positive or Gram-negative bacteria in specific points of the food processing and handling environment (more in Section 3.2).

2.1.3. Mechanisms of physicochemical inactivation. A variety of mechanisms are responsible for the MB activity of natural and synthetic nanopatterns. Ample experimental evidence has



(Caption appears on following page)

Figure 1 (Figure appears on preceding page)

Mechano-bactericidal (MB) nanotopographies: bactericidal mechanisms, property-activity relationships, and nanofabrication. (a) (i) Cicada wings (*Neotibicen pruinosus*) nanopillared patterns and (ii) *Pseudomonas aeruginosa* ruptured by the nanopillars (panel adapted with permission from Ivanova et al. 2012; copyright 2012 John Wiley & Sons). (b) Key parameters of nanopillared topographies (Linklater et al. 2020). (c) Primary MB mechanisms: (i) cell rupture by stretching and tearing, (ii) cell rupture by direct impaling, and (iii) sublethal mechanical damage inducing oxidative stress and apoptosis-like cell death. (d) 3D mapping of various synthetic MB nanopillars; the dashed circle in the lower left corner marks the dimensions of naturally occurring MB surfaces (panel adapted with permission from Linklater et al. 2020; copyright 2020 Nature Publishing Group). (e) (i) Nanoprotrusions generated by direct laser interference lithography and (ii) ruptured *Staphylococcus aureus* on this surface (panels adapted with permission from Cunha et al. 2016; copyright 2016 Elsevier). (f) (i) A profile view of ZnO nanocones generated by hydrothermal synthesis (inset: top view) and (ii) ruptured *Escherichia coli* on this surface (panels adapted with permission from Xie et al. 2020; copyright 2016 Elsevier). (g) (i) A profile view of polycarbonate nanocones formed by thermal nanoimprint lithography (inset: top view) and (ii) ruptured *E. coli* on this surface (panels adapted with permission from Cui et al. 2020; copyright 2020 ACS Publications). (h) (i) Nanotextured SS fabricated by electrochemical anodization and (ii) an *E. coli* cell adhered to that surface. (i) Negative templates with interpore distances of (i) 170 nm and (ii) 300 nm fabricated via electrochemical anodization; the nanocones in panel g were made from the 170-nm template via nanoimprint lithography (panels adapted with permission from Cui et al. 2020; copyright 2020 ACS Publications). Abbreviation: ROS, reactive oxygen species.

pointed to the rupture of the bacterial cell wall upon contact with nanostructures being the main cause of bacterial death, as suggested by observed deflated morphology and cytoplasm leakage from bacterial cells (Hawi et al. 2022, Linklater et al. 2020). The geometry (e.g., tip and base diameters, height) and spacing (either pitch or interspacing) of surface nanoprotrusions influence how the cell wall is ruptured (**Figure 1b**): Dense and blunt nanopillars tend to stretch and tear adhered bacteria (**Figure 1c**), whereas sparse and sharp ones tend to directly impale the cells (**Figure 1c**) (Michalska et al. 2018). Elasticity of nanostructures can intensify the tensile forces that stretch and tear the cell wall. For example, bendable nanoprotrusions such as silicon nanopillars [aspect ratio (AR) >10] and carbon nanotube forests (AR = 100–3,000) have been reported to kill bacteria via storage and release of mechanical energy incurred during bacterial adhesion (Ivanova et al. 2020, Linklater et al. 2018). Besides cell wall rupture, an alternative mode of Gram-negative cell wall disruption involves the separation of the cytoplasmic membrane from the cell wall, which may be mediated by adhesive EPSs and triggered by the forces originating from the movement of bacterial cells trapped on the crest of nanopillars (Bandara et al. 2017). Sublethal physico-mechanical disruptions may induce a bacterial stress response at the molecular level, which brings bacteria to their own demise. For example, induction of oxidative stress, elevated reactive oxygen species (ROS), and apoptosis-like death may occur in cells suffering sublethal mechanical injury (**Figure 1c**) (Jenkins et al. 2020, Zhao et al. 2022). The stress signals released by those directly affected by nanostructures might also induce programmed cell death in the neighboring cells not in direct contact with nanostructures (Durand & Ramsey 2019, Hayles et al. 2021). Moreover, transglycosylases, which are expressed to synthesize, remodel, or degrade the peptidoglycan layer for diverse purposes (e.g., for bacterial growth and division) (Dik et al. 2017), might partake in autolysis of bacterial cells after the initial deformation of the cell envelope, triggered by nanostructured surfaces (Mimura et al. 2022).

Complementary to experimental investigations, modeling approaches have also been used to fundamentally explain and quantify the physico-mechanical interactions between bacteria and nanostructures (Roy & Chatterjee 2021). The most representative are the thermodynamic (analytical) approach, which fits the first category, and the finite element (numerical) approach, which fits the latter (**Table 1**). The key concept underlying the thermodynamic approach is that system thermodynamic stability (i.e., free energy reduction) obtained via adsorption of a cell wall on the

Table 1 Mechano-bactericidal mechanisms and property–activity relationships revealed by analytical and numerical models as well as experiments

Area of focus	Thermodynamic/analytical models	Reference(s)	Finite element/numerical models	Reference	Experimental findings	Reference(s)
Location of cell wall rupture	Cell wall regions suspended between pillars	Pham et al. 2014, Pogodin et al. 2013	Cell wall regions against the apex of nanopillars Cell–nanopillar–liquid three-phase contact line near the apex	Velic et al. 2021 Cui et al. 2021	Experimental verification limited by insufficient resolution and lack of in situ, real-time imaging techniques	Roy & Chatterjee 2021
	Driving forces that pull bacteria toward nanoprotrusions	Pham et al. 2014, Pogodin et al. 2013	An evolving bond front between cell wall and nanoprotrusions Adhesion forces between cell surface and nanopillars	Velic et al. 2021 Cui et al. 2021		
Effect of nanoprotrusion height	Free energy reduction due to adsorption of cell wall onto nanopillars	Liu et al. 2019	Pressure of water column and gravity, applied on cell uniformly $H \approx 200$ nm	Mirzaali et al. 2018	Polycarbonate nanocones: critical height of nanopillars $H \approx 200$ nm, beyond which no difference in lethality to <i>Escherichia coli</i>	Cui et al. 2020
	A negative interfacial energy gradient down the nanopillars	Liu et al. 2019	Critical height of nanopillars $H \approx 200$ nm	Cui et al. 2021		
Effect of tip diameter	Uneven nanopillar heights resulting in greater stretching and killing (also supported by experimental findings in the same study)	Wu et al. 2018				
	In a slow-binding scenario, no association between tensile stress in the cell wall and d (range: 10–100 nm), in a fast-binding scenario, however, tensile stress increasing with d	Watson et al. 2019	Greater stress loading within cell envelope associated with smaller d ; $d < 100$ needed for rupturing <i>E. coli</i>	Cui et al. 2021	Polycarbonate nanocones: optimal killing of <i>E. coli</i> at $d \approx 45$ –60 nm, better than smaller or larger d	Cui et al. 2020
			Time-to-rupture decreasing with d Smaller d resulting in greater tip deflection and better bactericidal activity	Cui et al. 2021 L. Liu et al. 2018	ZnO nanopillars/cones: optimal killing of <i>E. coli</i> at smallest $d = 28.5$ nm Ni–Co-based nanocones/wires: optimal killing of <i>Salmonella enterica</i> at smallest $d = 5$ nm (range tested: 5–100 nm, supported by numerical simulation)	Xie et al. 2020 Liu et al. 2020

(Continued)

Table 1 (Continued)

Area of focus	Thermodynamic/analytical models	Reference(s)	Finite element/numerical models	Reference	Experimental findings	Reference(s)
Effect of pitch and interspacing	At fixed d , pressure on cells increasing with p (until cells become more likely to lie between nanopillars than encounter the tip of pillars); when $d = 60$ nm, $p > \sim 250$ nm is necessary for cell rupture	Liu et al. 2019	$IS > 300$ nm required for bactericidal activity against <i>Staphylococcus aureus</i>	Mirzaali et al. 2018	Polycarbonate nanocoines: optimal killing of <i>E. coli</i> observed at $p \approx 170$ nm (range: 100–300 nm)	Cui et al. 2020
		Ivanova et al. 2020, Linklater et al. 2018	Optimal p for nanopillars: 190–240 nm ($H = 200$ nm, $d = 40$ nm)	Cui et al. 2021	$C_{60}H_{18}Pt$ -based nanocoines: best killing of <i>S. aureus</i> occurred at $p \approx 190$ nm (range: 190–580 nm); orderliness of patterns had no impact	Modaresifar et al. 2020
Effect of mechanical properties	Cell rupture positively correlated with the deflection of nanopillars and the resultant elastic energy	Ivanova et al. 2020, Linklater et al. 2018	Stress distribution along nanopillars dependent on geometrical shape	L. Liu et al. 2018	Si nanopillars/carbon nanotubes: enhanced lateral stretching of bacterial cell wall (hence, more lethal to bacteria) from bendable nanopillars	Ivanova et al. 2020, Linklater et al. 2018
		Liu et al. 2019	Not explicitly considered or systematically studied in numerical models	NA	Si nanospikes: comparable bactericidal activity of hydrophilic and superhydrophobic nanospikes against <i>P. aeruginosa</i> and <i>S. aureus</i>	Linklater et al. 2017
Effect of surface chemistry	The more hydrophilic the surface (higher surface energy), the higher the bactericidal efficacy	Pogodin et al. 2013			Cicada wing nanopillars: surface chemical constituents and wettability important for bactericidal activity against <i>E. coli</i>	Román-Kustas et al. 2020

Abbreviations: d , diameter; H , nanopillar height; IS , interspacing; NA, not applicable; p , pitch.

surface of nanoprotusions incentivizes its deformation around them, which drives cells to engulf these nanostructures insofar as the energy cost due to bending and stretching of the cell wall can be compensated by the adhesion of the cell wall to the nanoprotusions (Liu et al. 2019, Pham et al. 2014, Pogodin et al. 2013). Rupture occurs when the cell wall is stretched beyond its local elastic limit, which is predicted to occur in the cell wall regions suspended between nanoprotusions (**Table 1**).

The finite element approach discretizes the cell wall and the crest of nanoprotusions into numerous tiny finite elements by applying a mesh and computes stress fields within each unit numerically (Roy & Chatterjee 2021). The finite element approach can accommodate a detailed cell wall model, including, for instance, laminates, each of them modeled with the specific mechanical properties of a constituent layer of the cell envelope. This has enabled a fairly accurate representation of the spatial distribution and temporal progression of mechanical stress and strain in a 3D cell wall while a bacterium is driven downward on nanoprotusions (Cui et al. 2021, Liu et al. 2020, Mirzaali et al. 2018, Velic et al. 2021).

Theoretical models have generated important insights into different aspects of physical interactions between bacteria and nanostructures, although disagreement remains regarding the driving force that pulls bacteria down against the nanoprotusions and the location of cell envelope rupture (**Table 1**). Additionally, experimental verification of model predictions remains extremely challenging: Despite recent advances in experimental techniques such as *ex situ* microscopic imaging, e.g., 3D reconstruction of the cell-nanostructure interface enabled by focused ion beam-scanning electron microscopy and transmission electron microscopy tomography (Bandara et al. 2017, Jenkins et al. 2020), we still lack imaging tools to capture or visualize the rapid progression of membrane rupture or tear, a process that occurs in minutes. Developments in super-resolution confocal microscopy that allows *in situ* optical sectioning of the cell-nanostructure interface, along with visualization of cell wall stretching via fluorescence resonance energy transfer (FRET), are likely to complement the *ex situ* techniques and provide further evidence for what occurs at the cell-surface interface, as well as MB model verification.

2.1.4. Property–activity relationships. Evidence accumulated so far suggests that MB activity is predominantly influenced by surface rather than bulk material properties, with topography being a leading factor, followed by mechanical properties and surface chemistry. As summarized in **Table 1**, numerous efforts have been made for probing and discovery of optimal MB designs, using both theoretical and experimental (isolation of factors) approaches. It is essential to recognize the great difficulty in identifying a set of surface properties—that is, a combination of topography, mechanical properties, and surface chemistry—that result in a global maximum in bactericidal activity because of the innumerable possible combinations. Along this line, it is then also important to generalize or extrapolate with caution the conclusions of experimental studies in terms of optimal designs (e.g., pillar height or pitch) for specific situations to other scenarios. Such optima may likely be local and contingent on the specific context of other surface properties that accompany the property of interest. For this reason, in **Table 1** we provided contextual information, such as materials involved, when presenting the experimental findings, to the extent that they were available in the original studies. Next, we highlight some noteworthy property–activity relationships observed so far without attempting to be exhaustive. Further readings on this topic can be found in recent reviews (Modaresifar et al. 2019, Roy & Chatterjee 2021).

The effects of topography have been more systematically studied than those of mechanical properties or surface chemistry. Modaresifar et al. (2019) compiled the results of various studies and reported general ranges of topographical parameters found to display MB activity against bacteria for various nanopatterns. Taking nanopillared surfaces as an example, typical topographies

with MB efficacy fall within heights of 100–900 nm, tip diameters of 20–207 nm, and interpillar spacing of 9–380 nm (see **Figure 1b** for illustration of the parameters). Remarkably, when mapping topographical parameters to a 3D space, an appreciable proportion of the synthetic nanopatterns found to have MB activity cluster closely with their natural counterparts (**Figure 1d**). Both modeling approaches and experimental evidence seem to agree on the existence of a critical height of ~200–300 nm for nanoprotusions, below which bactericidal activity improves with increasing height. Once that height is exceeded, no further improvement is expected or a reduction in activity may occur (**Table 1**). This is because the bacterial cell wall may contact the substratum if the height of nanoprotusions is not sufficient, preventing the overstretching necessary for rupture, whereas nanoprotusions that are too tall could result in clustering among neighbors, increasing effective diameters beyond what is optimal for MB activities.

The capability to change only one nanotopographical variable at a time in a systematic manner has driven the uncovering of property–activity relationships. For example, using deep ultraviolet (UV) immersion lithography, Ivanova et al. (2020) isolated the effect of a nanopillar height on antibacterial activity and found that compared to shorter (220 nm) or taller (420 nm) nanopillars, a pillar height of 360 nm exhibited the highest bactericidal efficacy toward both Gram-negative *Pseudomonas aeruginosa* (95% of cells were nonviable) and Gram-positive *Staphylococcus aureus* (83% of cells were nonviable). It was found that the intermediate height of 360 nm allowed storage of bacterial momentum as elastic potential energy in the deflected pillars, which in turn exerted lateral forces that stretch the cell wall to its rupture. Further increase of pillar height (420 nm), however, undermined bactericidal activity, as it became thermodynamically favorable for the neighboring pillars, which became increasingly pliable as height increased, to bundle up and form clusters, consequently reducing the tension on the bacterial cell wall. These results highlight how intricately coupled the topography, chemistry, and mechanical properties of nanostructured surfaces are, emphasizing the necessity of multifactorial data analysis and result interpretation. Aside from the height of nanoprotusions, the effects of other topographical parameters on MB activity have also been investigated, including tip diameter and pitch (or interspacing) (see references in **Table 1**), directionality (Elbourne et al. 2019), unevenness of height (Wu et al. 2018), orderliness of distribution (Modaresifar et al. 2020), etc.

Interactions between individual topographical parameters and their interplay with bacterial properties (e.g., cell wall structure, morphology, appendages) further complicate the quest for identifying an optimal MB design by only changing one variable at a time. Alternatively, a data-driven machine learning model (e.g., artificial neural network) was developed using an ensemble of experimental results in the literature to predict bactericidal performance against three bacterial strains, *E. coli*, *P. aeruginosa*, and *S. aureus* (Maleki et al. 2021). Once validated, the model was used to predict the optimal region in the topographical parameter space where excellent bactericidal activity is expected. The researchers found that the optimal regions vary among bacterial strains, but there exist overlaps where >85% bactericidal activity against all strains should be attainable (Maleki et al. 2021).

By comparison, only a limited number of studies so far have discussed the interaction between surface chemistry (wettability, surface energy, charge, etc.) and MB topographies, and this represents an underexplored avenue for future research in the MB field.

2.2. Nanofabrication of Mechano-Bactericidal Surfaces

The advances in modern nanofabrication technologies have enabled control over nanopattern construction with ever-increasing precision. For example, photolithography and electron-beam lithography have enabled direct nanoengineering as well as high-quality mask fabrication (i.e., indirect nanoengineering) with exceptional resolution (down to the sub-10-nm scale) and decoupled

topographical control (e.g., varying pillar height without changing pitch or diameter) (Chen et al. 2021, Ivanova et al. 2020). Despite their success in the electronics industry, application of these technologies for food industry applications is limited by high-cost, low-throughput challenges in patterning non-flat substrates or complex geometries and the requirement of specialized equipment or access to clean-room facilities. Additionally, their operation parameters have been optimized for semiconductor materials rather than materials commonly used for food applications (Hayles et al. 2021). Nanofabrication technologies that strike a balance between precision and practicality are more likely to be adopted by the food equipment or packaging manufacturing industries. In view of this, we next discuss a few of the most promising nanofabrication technologies that have the potential to address some of the challenges listed above.

2.2.1. Direct laser interference patterning. Direct laser interference patterning (DLIP, also known as laser interference lithography) utilizes ultrashort (femtosecond or picosecond) laser pulses to achieve maskless surface patterning. One prominent advantage of DLIP is its substrate versatility—it accurately ablates a wide range of materials without thermal damage (Meijer et al. 2002). DLIP has been demonstrated on SS (Du et al. 2022a, Wu et al. 2009), titania (Erdoğan et al. 2011), ceramics (Delgado-Ruíz et al. 2011), glass (Du et al. 2022a), and polymers (Aguilar et al. 2005). Direct nanopatterning of food-grade SS (304 or 316) is particularly attractive considering its widespread use in the food industry. One advantage of DLIP is that controlled topography can be readily obtained in a substrate-independent manner without the need for additional coatings or exposure to chemical etching, thus eliminating concerns about coating delamination and harmful chemical residues. Additionally, DLIP can achieve high patterning throughput with fast laser-scan speed (e.g., as high as 500 mm/s) and large laser-spot size (e.g., diameter $\sim 30 \mu\text{m}$) (Du et al. 2022a). Furthermore, because there is no boundary between the DLIP nanostructures and the bulk substrate, the resultant nanotopography is expected to be durable, which is essential to patterning large ($>1 \text{ m}^2$), high-wear surfaces like those encountered in food-handling environments. Nanopatterns such as nanoridges are attainable by a single laser line scan, and nanopillars are attainable by performing two laser line scans that intersect at a right angle (Cunha et al. 2016) (**Figure 1e**). Nevertheless, laser-induced nanostructures are currently limited by their blunt shape (i.e., tip diameter $> \sim 300 \text{ nm}$ and $\text{AR} < \sim 3$) because of insufficient decoupling of topographical parameters by DLIP (Peter et al. 2020), which may negatively impact their MB activity. For example, DLIP-treated SS (316L) featuring surface nanotopography of parallel ridges (peak-to-valley distance $\sim 150 \text{ nm}$ and width $\sim 1 \mu\text{m}$) exhibited only modest bactericidal activity ($\sim 25\%$) against both *E. coli* and *S. aureus* after 24 h of incubation, even in the presence of nonmechanical corroborating antibacterial factors such as the release of Ni ions (Du et al. 2022a). Smaller feature sizes may be attainable by using a laser source with shorter wavelengths or higher average powers (Peter et al. 2020). A method to ensure homogeneity of the nanopatterns generated by DLIP on non-flat surfaces should also be explored, as biofilms can also form on those surfaces (e.g., inner walls of pipelines, corrugated heat exchanger plates) and induce cross-contamination in the food processing environments.

2.2.2. Hydrothermal synthesis of metal oxide nanostructures. Hydrothermal synthesis (HS) of metal oxide nanostructures involves growing (poly)crystalline metal oxide nanostructures in an autoclave that provides pressurized and heated (typically $150\text{--}250^\circ\text{C}$) conditions. The growth of nanostructures can originate directly from an HS-compatible metal substrate without any coating step, or in the case of an arbitrary substrate, from an HS-compatible nanoparticle seed layer predeposited on its surface. This is a facile, scalable, and cost-effective process that yields controllable topographical features (e.g., tip diameter, height) by adjusting treatment temperature, time, pH, and concentration of additives (e.g., polyethyleneimine) (Chen et al. 2011, Jaggesar &

Yarlagadda 2020). Unlike DLIP, nanopatterning by HS is not confined by a line-of-sight radiation source (i.e., laser), enabling nanopatterning of objects of arbitrary shapes and/or microscale complexity. Nonetheless, nanotopographical HS relies on specific substrate material chemistries. The vast majority of research on hydrothermally synthesized MB nanotopography is based on titanium, titanium alloy, or zinc surfaces and is mostly focused on medical implant applications (e.g., dental, orthopedic) (Ishak et al. 2020). Although SS is relatively inert under hydrothermal conditions (Maslar et al. 2002), hydrothermal nanopatterning on SS can be achieved through seeded growth from surface-adsorbed nanoparticles (e.g., ZnO) (Xie et al. 2020, Yu et al. 2005). Other hydrothermally grown MB nanostructures include Ni-Co nanowires (Liu et al. 2020) and TiO₂ nanoblades (Wandiyanto et al. 2020) and nanospikes (Cao et al. 2018). Hydrothermally grown nanostructures comprising ZnO and TiO₂ also exhibit photocatalytic activities, generating ROS (e.g., superoxide anion, hydroxyl radicals, hydrogen peroxide) to complement the MB activity by introducing external oxidative stresses in addition to the internal stresses caused by cell envelope perturbation. This property can also be utilized to clean nanopatterned surfaces and restore their activity by the disintegration of surface-bound bacterial remnants. For example, Xie et al. (2020) showed that not only did ZnO nanocones (**Figure 1f**) exhibit fast bactericidal activity, with inactivation rates of 10⁷ and 10⁶ cells/(cm² · min) against *E. coli* and *S. aureus*, respectively, but also that 10 min of UV exposure mostly restored the bactericidal activity of the nanoarrays via photoinduced ROS production by ZnO. Notwithstanding the promising features, for HS to be adopted in food applications, the resulting nanopatterns need to be resilient under repeated mechanical impact or fluid shear stress and stable when exposed to acidic or alkaline solutions, as discussed in Section 3.4.

2.2.3. Nanoimprint lithography. Nanoimprint lithography (NIL) enables transfer of nanopatterns from nanostructured templates to a substrate (called a target in NIL, chiefly polymers) via direct mechanical deformation. Because of this, NIL is unbound by the resolution limits set by light diffraction or beam scattering. In fact, NIL is capable of generating sub-10-nm patterns (beneficial for the nanofabrication of sharp tips), achieving nanopatterns over large areas (e.g., via roll-to-roll processing), and reusing templates to reduce the fabrication costs (Ahn & Guo 2008, Chou & Krauss 1997). Three important criteria should be met by a target material for it to be compatible with NIL: (a) The material should be less stiff than the template; (b) the material should have a sufficiently low viscosity so that the imprinting process can be completed within a reasonable timeframe (Guo 2007); and (c) the material should yield under processing conditions but retain shape afterward. To meet these criteria, two types of NIL have been developed: thermal NIL and ultraviolet (UV) NIL. For thermal NIL, a polymeric target (often thermoplastic) is heated 70–90°C above its glass transition temperature (T_g) to reach a viscous flow state, followed by hot embossing, cooling below T_g , and template release (Guo 2007). Hard and durable templates have traditionally been made of Si, SiO₂, SiC, Si₃N₄, diamond, metals, or sapphire (Guo 2007). For UV NIL, UV-curable precursors are used; because of their intrinsically low viscosity, the nanoimprinting and curing can be carried out at ambient temperatures. Nevertheless, one restriction of UV NIL is that either the template or the target must be UV transmissible to achieve efficient curing. Evaporation of solvent from a solvated polymer matrix represents a third method to stiffen the NIL-imprinted nanostructures. For example, polysaccharide-based nanocones have been achieved by evaporating 2-butanone (solvent) from solubilized oligoglucosamine (polymer) using a γ -cyclodextrin-based template (Park et al. 2019a, Takei & Yasuda 2020). Notably, for evaporation NIL, templates made of porous materials (e.g., cyclodextrin-based) may further improve the sharpness of tips or edges of the imprinted nanofeatures by allowing solvent (or air) entrapped in the interstitial space between the template and the target to escape (Takei & Hanabata 2015).

Despite the abovementioned material requirements, NIL can confer various nanopatterns on a wide range of soft, flexible materials (elastic modulus $\sim 0.04\text{--}4$ GPa) (Linklater et al. 2022, Tan et al. 2020). Promising MB nanoprotusions, such as nanopillars and nanocones, have been achieved through NIL on a variety of commercial plastic films [e.g., polycarbonate, poly(methyl methacrylate), poly(ethylene glycol diacrylate), nylon, poly(ethylene terephthalate), polyethylene, and polypropylene; see **Figure 1g**] as well as lignocellulosic biopolymers (e.g., cellulose acetate, hydroxypropyl cellulose, oligoglucosamine, lignin) (Cui et al. 2020, Dickson et al. 2015, Espinha et al. 2018, Linklater et al. 2022, Park et al. 2019a, Takei & Yasuda 2020, Tan et al. 2020, Worgull et al. 2013). Templates such as anodic aluminum oxide substrates with conical pores and silicon nanopillars (formed by reactive ion etching with colloidal particle masks) have been used for nanoimprinting onto these flexible substrates (Cui et al. 2020, Linklater et al. 2022, Tan et al. 2020). For these soft and flexible nanopatterns, loss of fidelity over time due to processes like creep may be a potential challenge (e.g., for food-packaging applications) and should be further investigated. The NIL-enabled nanostructured surfaces can be used directly or serve as resists for further pattern transfer via wet (e.g., hydrofluoric acid) or dry etching (e.g., reactive ion etching, ion milling) (Chen 2015). The latter may represent one viable strategy to confer MB nanopatterns on stiffer materials that are not amenable to NIL otherwise, such as food-grade SS (~ 190 GPa).

2.2.4. Electrochemical anodization. Electrochemical anodization (EA) drives the anodic growth of ordered cylindrical pores from metallic substrates, which typically happens in the presence of oxidizing electrolytes and under an applied electric field. Similar to HS, anodization allows for nanostructuring of metallic substrates of arbitrary curvatures and geometries over a large surface area. Furthermore, it also offers precise and independent control over multiple nanotopographical features across a wide range (e.g., pore diameter, 6–500 nm; pore length, tens of nm to hundreds of microns; and a variety of pore shapes) via tunable anodization parameters (Cheng & Yang 2021, Masuda et al. 2001, Sulka 2008). To date, the antifouling properties of porous anodic materials (e.g., alumina, titania) against food pathogens are better known than their MB activities (Feng et al. 2014, 2015, 2019). In one study, Jang et al. (2018) obtained nanopikes on SS 316L via EA in nitric acid and demonstrated their bactericidal activity against *E. coli* while preserving cytocompatibility with mammalian cells (**Figure 1b**). Intriguingly, such MB activity was achieved without visibly rupturing the *E. coli* cells (**Figure 1b**), possibly because of the height of the nanopikes (average roughness ~ 5 nm) being less than the typical thickness of a Gram-negative cell wall (~ 50 nm). Additionally, anodic SS surfaces exhibit improved corrosion resistance due to Cr and Mo enrichment on the surface, which could be a beneficial property for many food-contact surfaces (Jang et al. 2018). As noted in Section 2.2.3, EA may serve as a scalable, high-throughput, and cost-effective method to manufacture large templates for NIL-based MB surfaces. For example, through recursive anodization and pore widening, one can obtain ordered arrays of inverted conical voids as a negative mold that, upon nanoimprinting on a deformable soft material, produces nanocones/nanopillars with MB activity (**Figure 1f**) (Cui et al. 2020, Linklater et al. 2022).

One prominent advantage of anodic nanopatterning over other nanofabrication technologies is that industrial-scale anodization infrastructure is well-established for passivation and coloring purposes and could be repurposed for producing MB materials. Moreover, in terms of material safety, both alumina and titania have been considered safe food-contact substances by the US Food and Drug Administration. These considerations afford anodic nanopatterning a high-technology-readiness level for food applications. Nonetheless, similar to HS-induced nanostructures, the durability of anodic metal oxide under repeated exposure to an acid or base should be carefully examined before they can be used as food-contact surfaces (see additional discussion in Section 3.3).

2.2.5. Orthogonal nanoengineering. Designing MB nanopatterns that consistently achieve above 2-log reduction (99%) of both Gram-positive and Gram-negative strains remains a challenge despite progress on nanotopographical optimization (Linklater & Ivanova 2022). To enhance the bactericidal efficacy of MB nanopatterns, surface properties that are independent of nanotopography should be systematically investigated and leveraged. These surface properties include, among others, wettability, charge, or bioactivity. Given that MB efficacy is sensitive to even the slightest change in nanotopography (see Section 2.1.4), introducing these properties without adversely affecting the desired nanotopographies is critical and remains a technical challenge.

Orthogonal nanoengineering (ONE) may provide a solution to this challenge. ONE is a nanofabrication concept focused on enabling decoupled engineering control over the aforementioned surface properties with nanoscale precision (Cheng & Yang 2021). As noted in Section 2.2, most nanofabrication methods that hold potential for food applications are restricted to certain materials and their inherent surface properties (e.g., HS to ZnO or TiO₂). Thus, a sequential nanoengineering scheme may prove practical and effective in achieving orthogonal control: First, MB nanotopography can be formed on materials compatible with the chosen nanofabrication method, followed by application of ultrathin coatings (<20 nm) to introduce desired functional moieties atop the nanostructured native materials while keeping the beneficial topographical features intact. The scope of surface chemistry modification can go beyond hydrophilicity/hydrophobicity, which has been the main focus of previous investigations on the effect of surface chemistry on MB activity (Linklater et al. 2017). Surface charges (including zwitterionic moieties), electrical or ionic conductivity, and stimuli responsiveness (e.g., pH, temperature, salinity, and relative humidity) can be conferred to native materials via coatings (Alf et al. 2010, Coclite et al. 2013, Gleason 2020, Yang et al. 2012). With the assistance of surface chemistry-derived properties introduced via ONE, the orthogonally nanoengineered MB (ONE-MB) efficacy can be improved in two major ways: (a) prolonging MB activity, especially important for high-fouling environments encountered in food applications, and (b) enhancing overall bactericidal efficacy by combining a multitude of antibacterial modes.

A few pioneering studies have demonstrated the potential of ONE in sustaining the bactericidal activity of MB nanopatterns. For example, antifouling-bactericidal dual functionality can be achieved by decorating MB nanopatterns with zwitterionic polymer coatings (Park et al. 2019a,b). Kill-release is another promising strategy. Dislodging cellular remnants from dead bacteria from the bactericidal nanofeatures is crucial to their renewal and sustained activity. This has been achieved by activating the coatings (e.g., swelling) through a variety of environmental stimuli such as exposure to salt, enabled by salt-responsive polyzwitterionic brushes grafted on NIL nanocones (Liu et al. 2022), alternating between wet and dry states (Yi et al. 2022), or temperature cycling (for thermoresponsive polymer coated on HS nanocones) (Jiang et al. 2021). Although unexplored in the context of ONE-MB, coating activation has been attained via light exposure or pH change on flat surfaces (Gleason 2020, Unger et al. 2017). All the aforementioned stimuli are typically present in food-handling environments and could therefore be leveraged to trigger the release of bacteria remnants or other debris and prolong the lifetime of MB nanopatterns modified via ONE.

Aside from sustaining bactericidal activity, ONE holds promise for enhancing the overall bactericidal activity via three mechanisms. First, surface energy and positive charge density of the MB nanostructures can be tuned to augment the cell wall nanostructure attractive interaction, which in turn improves the likelihood of rupturing the bacterial cell wall (L. Liu et al. 2018, 2019, Pogodin et al. 2013). Second, enhanced killing may also be attainable synergistically by integrating a membrane-damaging chemical species. Antimicrobial chemistries, such as lipophilic or positively charged moieties, can be conferred to MB nanopatterns via an ultrathin coating

(Martin et al. 2007, Tiller et al. 2001, Tu et al. 2013, Yuan & Zhang 2017). Likewise, bioactive macromolecules, such as bacteriocins or lysozymes, can be immobilized on the nanopatterns. Synergistic enhancement can be expected when the MB mechanism complements the biochemical one. For example, bactericidal activity against Gram-positive strains may be improved with lysozymes immobilized on nanoprotusions, as the enzymes may hydrolyze the glycosidic bonds in the bacterial peptidoglycan layer (Khlyustova et al. 2022). This can weaken its tensile strength and make it easier to rupture during physicochemical stretching. Moreover, the increased curvature at the crests of nanoprotusions may further promote the activity and stability of the immobilized enzymes (Talbert & Goddard 2013). A third mechanism is through accelerating the release kinetics of biocides due to enlarged specific surface area afforded by the nanoprotusions. This concept has been demonstrated using two systems: Ag nanoparticles deposited on laser-patterned metallic glass (Du et al. 2022b) and gentamicin-releasing ultrathin coating on anodized titanium oxide with hierarchical nanostructures (Hizal et al. 2015). Furthermore, nanozymes (metal/metal oxide nanoparticles with catalytic activity) and organocatalysts (small organic molecules with catalytic activity) that are capable of converting bacterial metabolites into antimicrobials (e.g., H₂O₂, hypobromous acid) can also be immobilized on MB nanopatterns for synergistic inactivation (Lang et al. 2022, Mousavi et al. 2021, Negut et al. 2018, Nishiyama et al. 2014, Sundara Selvam et al. 2020). The bacteria-triggered local release of antimicrobials is attractive for food applications, as it can limit unintended release of antimicrobial agents into food and thus minimize adverse effects on food safety and quality.

To date, the majority of the existing ONE-MB were made through solution-based techniques such as dip/spin coating, layer-by-layer assembly, self-assembled monolayers, electroplating, and inject printing; their applications in antimicrobial food equipment coatings have been reviewed by Bastarrachea et al. (2015). By comparison, vapor-phase techniques, such as chemical vapor deposition (CVD), have enabled ultrathin coatings with nanoscale precision in the absence of solvent, which circumvents several issues common in solution-based techniques such as pinholes, nonuniformity, contamination, and solvent toxicity. In particular, initiated CVD (iCVD) is well-suited for conferring antifouling (Chen et al. 2022, Donadt & Yang 2021), antimicrobial (Martin et al. 2007), or bacterial virulence-modulating properties on a wide variety of substrates (Franklin et al. 2021), including heat-sensitive plastic, paper, and textile substrates, due to a low substrate temperature requirement, generally around room temperature. Moreover, iCVD supports a high retention of monomer functional moieties, a rich chemical library (>70 functional monomers), a high deposition rate (>200 nm/min), multiscale thickness control (a few nm to tens of μm), conformal coverage of complex and high-aspect-ratio nanostructures (Asatekin & Gleason 2011, Cheng et al. 2020, Coclite et al. 2013, Gleason 2021, Reeja-Jayan et al. 2014), and long-term durability even under elevated temperatures (Paxson et al. 2014). Additionally, iCVD is compatible with economical roll-to-roll manufacturing (Gleason 2020, Gupta & Gleason 2006), facilitating facile integration with production lines for flexible food packaging at industrial scale. Comparisons of these various vapor-phase coating methods for biointerface applications are covered elsewhere (Franklin & Yang 2020, Khlyustova et al. 2020).

3. CHALLENGES AND OPPORTUNITIES FOR FOOD APPLICATIONS

MB surfaces represent an emerging intervention strategy for mitigating the serious biofilm problems faced by the food industry. Their physicochemical inactivation mechanisms are different than those of traditional biocide-based strategies and thus have significant potential for a nonleaching, long-lasting biofilm control approach for material surfaces encountered in food-handling environments. The fast rate of progress on precise but practical nanofabrication technologies (i.e., those that are cost-effective, scalable, accommodating various material types

and shapes) further boosts the likelihood of MB surfaces making a real impact in the coming years. However, some challenges still need to be addressed to realize the potential of MB surfaces in food applications, and these are discussed below.

3.1. Evaluation of Mechano-Bactericidal Efficacy

Methods for evaluating the efficacy of MB surfaces need to be standardized and should reflect the intended use scenarios in the food industry to determine their true potential and limitations. Generally, two testing methods are used to evaluate bactericidal efficacy: (a) immersion of test coupons containing MB nanostructures in bacterial suspension (Ivanova et al. 2012) and (b) dispensing droplets of bacterial suspension on the surface of test coupons (Valiei et al. 2020). Large discrepancies in effectiveness could result from the same nanopattern under these different incubation settings: Specifically, the latter has been shown to induce much higher bactericidal activity due to the moving air–liquid–solid triple interface at the periphery of evaporating droplets, which in turn supplies additional capillary pull that drives cells into nanopillars (Valiei et al. 2020). Both solid–liquid and triple interfaces are relevant for food applications. For example, surfaces of pipes or valves in liquid food processing are likely to be fully immersed in liquid foods or cleaning solutions and for these the immersion method provides a more accurate evaluation, whereas surfaces of a deli meat slicer or a conveyor belt are more likely to encounter liquid droplets, for which the second method is more appropriate. Furthermore, proof-of-concept studies conducted in buffers or culture media should be followed by validation studies in real food matrices (or close analogs) encountered in the intended applications, because bacterial resistance to MB nanopatterns could depend on food components. For instance, Mimura et al. (2022) reported that 10 mM of Mg^{2+} drastically improved the tolerance of *E. coli* cells to MB nanopillars, possibly due to inhibition of the bacterial autolytic process by Mg^{2+} (Leduc et al. 1982). This concentration of Mg^{2+} is comparable to that of many liquid foods, such as soy milk (~7 mM) and whole milk (~5 mM). Additionally, conditioning film formation and flow rates for the intended food application should also be closely mimicked in the laboratory screening of MB surfaces (Michalska et al. 2021, Sjollema et al. 2018). Finally, these novel surfaces should be tested in practical settings of food processing, packaging, and service environments to establish their real-world effectiveness (Yamada et al. 2018). This requires a close collaboration between research institutions and food and packaging companies as well as regulatory agencies (Robertson 2013).

3.2. Efficacy Against Gram-Positive Bacteria

As discussed in Section 2.1.2, the efficacy of MB surfaces is generally lower against Gram-positive compared to Gram-negative bacteria. This could be problematic because many Gram-positive bacteria cause both food safety (e.g., *Listeria monocytogenes*, *Bacillus cereus*, *S. aureus*) and food quality (e.g., *Bacillus licheniformis*, *Geobacillus* spp., *Lactobacillus* spp.) issues. In particular, *L. monocytogenes* is known for its ability to persist in ready-to-eat food processing plants on both food-contact (e.g., equipment, utensils, instruments) and non-food-contact (e.g., drains, floors, cart wheels) surfaces for prolonged periods, even months to years, causing repeated contamination of food products (Thimothe et al. 2004). Furthermore, many Gram-positive bacteria (e.g., *Bacillus cereus*) also form spores that are highly resistant to environmental stresses, including wet and dry heat, desiccation, toxic chemicals, and radiation (Setlow 2007), and as a result can survive a variety of inactivation or disinfection steps during food processing. Encouragingly, MB activities against *Bacillus subtilis* spores have been demonstrated on both dragonfly wings and black silicon (Ivanova et al. 2013). More validation studies on foodborne spoilage (e.g., *Geobacillus* spp., *Bacillus licheniformis*) and/or pathogenic spore formers (e.g., *Bacillus cereus*, *Clostridium perfringens*, *Clostridium botulinum*) are

necessary to establish MB surfaces as an effective way to control spores in food-handling environments (Scheldeman et al. 2006). Synergistic enhancement of bactericidal activity via ONE (see Section 2.2.5) should also be explored to overcome the lack of efficacy against Gram-positive bacteria.

3.3. Effective Distance of Mechano-Bactericidal Activity

The nonmigratory nature of MB surfaces creates a short effective range/distance, which could be further diminished by masking of nanopatterns by food components and/or remnants from killed bacteria. Primary food packaging, which is the packaging in direct contact with the food product, has been proposed as a potential target for MB surface nanopatterns (Linklater et al. 2022). In light of the limited effective distance afforded by MB surfaces, two scenarios may be considered for the effectiveness of nanopatterning for food-packaging materials: (*a*) before the packaging step, for reducing the risk of bacterial contamination of the packaging material itself, and (*b*) after the packaging step, for inactivating foodborne bacteria on the surface of the packaged food. Based on the earlier mechanistic discussion, MB nanopatterns could offer protection against contamination of the packaging materials with bacteria of human or environmental origin (Scenario *a*), thus lowering the risk of cross contaminating the food products. Nevertheless, cost-benefit and life-cycle analyses should be conducted to evaluate whether it is feasible to use MB nanopatterned materials to supplement or replace current surface decontamination methods such as light-based or chemical treatments.

As for Scenario *b* (in-package decontamination), liquid and solid foods need to be discussed separately. For liquid foods, the proportion of bacteria in the packaged liquid food or beverage that comes in contact with the surface-bound nanopattern may be small. Factors that facilitate their contact, such as the conditioning film, diffusion, bacterial motility, and convective flow, may determine the overall effectiveness of the MB nanopatterns as an in-package antimicrobial hurdle. For solid foods, the effectiveness of MB nanopatterned materials against food surface microflora depends on the surface area in direct contact with the MB nanopatterns. Therefore, films used in vacuum packaging of foods with relatively smooth surfaces, such as cheeses and meats, could be good candidates for applying NIL-enabled MB nanopatterns. However, it should be noted that even 100% contact on a macroscopic scale could still leave bacteria hiding in microscopic crevices and folds untouched by the killing nanopatterns. This is one of the limitations of these surfaces, and thus they should be used as an additional hurdle rather than the sole antimicrobial barrier.

3.4. Long-Term Durability of Nanostructured Surfaces

Long-term durability of nanostructures under conditions encountered in food processing, packaging, and service environments is crucial to their lifetime and affordability. Such conditions include, but are not limited to, repeated exposure to mechanical (abrasion, shear stress under flow), chemical (acidic, alkaline, oxidizing, saline), thermal (steam, freezing), and/or irradiation (UV, pulsed light) treatments. Although sharp-edged surfaces (especially tip diameter < 60 nm) tend to afford greater bactericidal activity (Cui et al. 2021, Han et al. 2018), their repeated exposure to mechanical stress may result in morphological changes or even nanostructure break-off. The latter renders the surface less effective over time but may also introduce potentially harmful nanomaterials into foods (Eleftheriadou et al. 2017, Kwiatkowski et al. 2020); rigorous testing of the robustness of MB nanopatterns must be carried out under levels of mechanical stresses typical for food manufacturing and handling scenarios. For example, testing under turbulent flow regimes should be required to validate suitability for use in food-contact surfaces such as pipe walls or heat exchanger plates (Li et al. 2019). Equally important is surface feature durability under frequent mechanical

impact and/or abrasion, which is highly relevant for the surfaces of conveyer belts, chutes, knives, etc. (DeFlorio et al. 2021). Therefore, application-specific mechanical challenge studies, such as shear abrasion, bending, and impact tests, should be performed on those nanopatterned surfaces (Nyankson et al. 2022). Promisingly, some early work has shown that MB nanotopographies may meet the demand for mechanical durability. For example, Hasan et al. (2020) reported that bactericidal nanoblades generated by wet-etching of Al could sustain 1,000 cycles of load pressure of 6.4 MPa, which is orders of magnitude higher than the average pressure of 250 KPa applied by hand when working with tools, without any detectable topography damage (Hasan et al. 2020). Furthermore, in light of the potentially high cytotoxicity of high-aspect-ratio nanoparticles (Piret et al. 2012), the quantity and morphology of mechanically dislodged nanoparticles must be meticulously characterized, their environmental fate tracked, and cytotoxicity examined in both in vitro and in vivo models (Abdolahpur Monikh et al. 2019, Mattsson et al. 2017, Sukhanova et al. 2018, Wagner & Reemtsma 2019).

Chemical durability of nanostructured surfaces during exposure to acidic foods and/or cleaning solutions of extreme pH (acidic or alkaline) has important safety and quality implications and must also be examined. In particular, MB surfaces composed of metal or metal oxide, such as those fabricated by DLIP, HS, and EA, may be unstable under acidic or alkaline conditions and introduce contaminants via dissolution. For example, ZnO-based nanospikes may dissolve quickly under acidic conditions, especially at pH 4.6 or lower, which may limit its application as a food-contact surface for acidic foods and/or preclude cleaning with acidic sanitizers (Fruhwrth et al. 1982, C.F. Liu et al. 2018). Furthermore, some liquid foods contain acids that are strong metal complexing agents (e.g., citric acid), which could gradually damage the nanostructures while releasing metal ions or metal complexes into food, raising concerns over adverse organoleptic changes (Mazinanian et al. 2015). Thus, to identify suitable food-contact applications for MB surfaces, it is crucial to conduct long-term (weeks to months) exposure studies using a range of foods or food simulants and actual cleaning agents used in the food industry. As for plastic-based nanostructures, such as those formed by NIL, material responses to thermal and irradiation treatments should also be carefully evaluated.

4. CONCLUSIONS AND OUTLOOK

Since the first reports of MB phenomena observed on cicada wings just a decade ago, remarkable progress has been made in elucidating their bactericidal mechanisms and developing a variety of practical, synthetic nanofabricated analogs. Although progress to date is very encouraging, much more work is needed before the large-scale adoption of nanostructures for food applications. Future research on the nanofabrication of MB surfaces for food applications may encompass: (a) maskless, direct nanofabrication with improved nanotopographical control; (b) cost-effective nanofabrication of large masks/templates that maintain their nanotopographical fidelity over repeated use; (c) masks/templates compatible with roll-to-roll printing of MB nanopatterns; (d) broadening substrate categories of nanofabrication to involve common food-contact materials (e.g., SS, cellulosic materials, rubbers); and (e) ONE for further improvement of bactericidal activity and long-term effectiveness of MB surfaces. Although most efforts have focused on bactericidal surfaces, viruses and fungi are also omnipresent in food-handling environments and can cause food safety and quality issues. Viruses and fungi are very different from bacteria in size, morphology, and envelope structure, which will likely affect the efficacy of physicochemical inactivation mechanisms of nanostructures against these microbes. This represents an unexplored opportunity for future research on mechano-microbiocidal surfaces.

Cleanability of MB surfaces is an important criterion for their successful implementation in the food industry. Mild but effective cleaning strategies may be developed, tailored to the specific

needs of nanoengineered MB surfaces. For example, a cleaning scheme that involves gentle cycling of temperature or salinity under flow around the actuation point could facilitate the removal of surface-adsorbed bacterial remnants or biomolecules masking the ONE-MB nanopatterns. This would, however, require the rest of the process line to be cleanable by the same scheme as well (e.g., in a clean-in-place scenario), thus highlighting the importance of taking a holistic approach when implementing nanoengineered surfaces.

An important step forward for MB materials is the translation of benchtop success to applications that have positive implications for human life, including food applications. Continuous multidisciplinary efforts spanning chemistry, microbiology, biophysics, nanoengineering, material science, toxicology, and food science, and collaborations across academia, industry, and regulatory agencies are key to realizing the full potential of MB in the food industry. In our opinion, MB surfaces can be part of the solution against undesirable microorganisms and microbial biofilms in the food sector and may help enhance food safety and quality. Optimal outcomes may only manifest when these emergent materials are implemented in tandem with other measures that prevent microbial proliferation in food manufacturing and handling, including hygienic design of food processing equipment and well-designed and executed food safety plans.

DISCLOSURE STATEMENT

The authors are not aware of any affiliations, memberships, funding, or financial holdings that might be perceived as affecting the objectivity of this review.

ACKNOWLEDGMENTS

This material is based on work supported by the Department of the Navy, Office of Naval Research under ONR award N00014-20-1-2418 to R.Y., USDA-NIFA Award 2021-67034-35040 to Y.C., and USDA-NIFA Award 65210-20024-11 to C.I.M. It is also based on work supported by the National Science Foundation Graduate Research Fellowship Program under grant DGE-1650441. Any opinions, findings, conclusions, or recommendations expressed in this material are those of the author(s) and do not necessarily reflect the views of the National Science Foundation or the USDA.

LITERATURE CITED

- Abdolahpur Monikh F, Grundschober N, Romeijn S, Arenas-Lago D, Vijver MG, et al. 2019. Development of methods for extraction and analytical characterization of carbon-based nanomaterials (nanoplastics and carbon nanotubes) in biological and environmental matrices by asymmetrical flow field-flow fractionation. *Environ. Pollut.* 255:113304
- Aguilar CA, Lu Y, Mao S, Chen S. 2005. Direct micro-patterning of biodegradable polymers using ultraviolet and femtosecond lasers. *Biomaterials* 26(36):7642–49
- Ahn SH, Guo LJ. 2008. High-speed roll-to-roll nanoimprint lithography on flexible plastic substrates. *Adv. Mater.* 20(11):2044–49
- Alf ME, Asatekin A, Barr MC, Baxamusa SH, Chelawat H, et al. 2010. Chemical vapor deposition of conformal, functional, and responsive polymer films. *Adv. Mater.* 22(18):1993–2027
- Asatekin A, Gleason KK. 2011. Polymeric nanopore membranes for hydrophobicity-based separations by conformal initiated chemical vapor deposition. *Nano Lett.* 11(2):677–86
- Bandara CD, Singh S, Afara IO, Wolff A, Tsefamichael T, et al. 2017. Bactericidal effects of natural nanotopography of dragonfly wing on *Escherichia coli*. *ACS Appl. Mater. Interfaces* 9(8):6746–60
- Bastarrachea LJ, Denis-Rohr A, Goddard JM. 2015. Antimicrobial food equipment coatings: applications and challenges. *Annu. Rev. Food Sci. Technol.* 6:97–118
- Beveridge TJ. 1999. Structures of gram-negative cell walls and their derived membrane vesicles. *J. Bacteriol.* 181(16):4725–33

- Cao Y, Su B, Chinnaraj S, Jana S, Bowen L, et al. 2018. Nanostructured titanium surfaces exhibit recalcitrance towards *Staphylococcus epidermidis* biofilm formation. *Sci. Rep.* 8(1):1071
- Chen LY, Yin YT, Chen CH, Chiou JW. 2011. Influence of polyethyleneimine and ammonium on the growth of ZnO nanowires by hydrothermal method. *J. Phys. Chem. C* 115(43):20913–19
- Chen P, Lang J, Zhou Y, Khlyustova A, Zhang Z, et al. 2022. An imidazolium-based zwitterionic polymer for antiviral and antibacterial dual functional coatings. *Sci. Adv.* 8(2):eabl8812
- Chen Y. 2015. Applications of nanoimprint lithography/hot embossing: a review. *Appl. Phys. A* 121(2):451–65
- Chen Y, Shu Z, Zhang S, Zeng P, Liang H, et al. 2021. Sub-10 nm fabrication: methods and applications. *Int. J. Extreme Manuf.* 3(3):032003
- Cheng Y, Feng G, Moraru CI. 2019. Micro- and nanotopography sensitive bacterial attachment mechanisms: a review. *Front. Microbiol.* 10:191
- Cheng Y, Khlyustova A, Chen P, Yang R. 2020. Kinetics of all-dry free radical polymerization under nanoconfinement. *Macromolecules* 53(24):10699–710
- Cheng Y, Yang R. 2021. Toward programming bacterial behavior via synthetic interfaces: physicochemical nanopatterning, decoupling surface properties, and integrating material and biological insights. *Acc. Mater. Res.* 2(11):979–85
- Chou SY, Krauss PR. 1997. Imprint lithography with sub-10 nm feature size and high throughput. *Microelectron. Eng.* 35(1–4):237–40
- Coclitte AM, Howden RM, Borrelli DC, Petruczuk CD, Yang R, et al. 2013. 25th anniversary article: CVD polymers: a new paradigm for surface modification and device fabrication. *Adv. Mater.* 25:5392–423
- Cools I, Uyttendaele M, Cerpentier J, D’Haese E, Nelis HJ, Debevere J. 2005. Persistence of *Campylobacter jejuni* on surfaces in a processing environment and on cutting boards. *Lett. Appl. Microbiol.* 40(6):418–23
- Cui Q, Liu T, Li X, Song K, Ge D. 2020. Nanopillared polycarbonate surfaces having variable feature parameters as bactericidal coatings. *ACS Appl. Nano Mater.* 3(5):4599–609
- Cui Q, Liu T, Li X, Zhao L, Wu Q, et al. 2021. Validation of the mechano-bactericidal mechanism of nanostructured surfaces with finite element simulation. *Colloids Surf. B* 206:111929
- Cunha A, Elie AM, Plawinski L, Serro AP, Botelho do Rego AM, et al. 2016. Femtosecond laser surface texturing of titanium as a method to reduce the adhesion of *Staphylococcus aureus* and biofilm formation. *Appl. Surf. Sci.* 360:485–93
- De Geyter J, Tsirigotaki A, Orfanoudaki G, Zorzini V, Economou A, Karamanou S. 2016. Protein folding in the cell envelope of *Escherichia coli*. *Nat. Microbiol.* 1:16107
- DeFlorio W, Liu S, White AR, Taylor TM, Cisneros-Zevallos L, et al. 2021. Recent developments in antimicrobial and antifouling coatings to reduce or prevent contamination and cross-contamination of food contact surfaces by bacteria. *Compr. Rev. Food Sci. Food Saf.* 20(3):3093–134
- Delgado-Ruiz RA, Calvo-Guirado JL, Moreno P, Guardia J, Gomez-Moreno G, et al. 2011. Femtosecond laser microstructuring of zirconia dental implants. *J. Biomed. Mater. Res. B* 96(1):91–100
- Dickson MN, Liang EI, Rodriguez LA, Vollereaux N, Yee AF. 2015. Nanopatterned polymer surfaces with bactericidal properties. *Biointerphases* 10(2):021010
- Dik DA, Marous DR, Fisher JF, Mobashery S. 2017. Lytic transglycosylases: concinnity in concision of the bacterial cell wall. *Crit. Rev. Biochem. Mol. Biol.* 52(5):503–42
- Donadt TB, Yang R. 2021. Amphiphilic polymer thin films with enhanced resistance to biofilm formation at the solid–liquid–air interface. *Adv. Mater. Interfaces* 8(5):2001791
- Du C, Wang C, Zhang T, Zheng L. 2022a. Antibacterial performance of Zr-BMG, stainless steel, and titanium alloy with laser-induced periodic surface structures. *ACS Appl. Bio Mater.* 5(1):272–84
- Du C, Yang Y, Zheng L, Zhang T, Zhao X, Wang C. 2022b. Structure-element surface modification strategy enhances the antibacterial performance of Zr-BMGs. *ACS Appl. Mater. Interfaces* 14(7):8793–803
- Durand PM, Ramsey G. 2019. The nature of programmed cell death. *Biol. Theory* 14(1):30–41
- Elbourne A, Coyle VE, Truong VK, Sabri YM, Kandjani AE, et al. 2019. Multi-directional electrodeposited gold nanospikes for antibacterial surface applications. *Nanoscale Adv.* 1(1):203–12
- Eleftheriadou M, Pyrgiotakis G, Demokritou P. 2017. Nanotechnology to the rescue: using nano-enabled approaches in microbiological food safety and quality. *Curr. Opin. Biotechnol.* 44:87–93

- Erdoğan M, Öktem B, Kalaycıoğlu H, Yavaş S, Mukhopadhyay PK, et al. 2011. Texturing of titanium (Ti6Al4V) medical implant surfaces with MHz-repetition-rate femtosecond and picosecond Yb-doped fiber lasers. *Opt. Express* 19(11):10986
- Espinha A, Dore C, Matricardi C, Alonso MI, Goñi AR, Mihi A. 2018. Hydroxypropyl cellulose photonic architectures by soft nanoimprinting lithography. *Nat. Photonics* 12(6):343–48
- Feng G, Cheng Y, Wang S, Borca-Tasciuc DA, Worobo RW, Moraru CI. 2015. Bacterial attachment and biofilm formation on surfaces are reduced by small-diameter nanoscale pores: How small is small enough? *npj Biofilms Microbiomes* 1:15022
- Feng G, Cheng Y, Wang S, Hsu LC, Feliz Y, et al. 2014. Alumina surfaces with nanoscale topography reduce attachment and biofilm formation by *Escherichia coli* and *Listeria* spp. *Biofouling* 30:1253–68
- Feng G, Cheng Y, Worobo RW, Borca-Tasciuc DA, Moraru CI. 2019. Nanoporous anodic alumina reduces *Staphylococcus* biofilm formation. *Lett. Appl. Microbiol.* 69(4):246–51
- Frank JF, Koffi RA. 1990. Surface-adherent growth of *Listeria monocytogenes* is associated with increased resistance to surfactant sanitizers and heat. *J. Food Prot.* 53(7):550–54
- Franklin T, Wu Y, Lang J, Li S, Yang R. 2021. Design of polymeric thin films to direct microbial biofilm growth, virulence, and metabolism. *Biomacromolecules* 22(12):4933–44
- Franklin T, Yang R. 2020. Vapor-deposited biointerfaces and bacteria: an evolving conversation. *ACS Biomater. Sci. Eng.* 6(1):182–97
- Fruhwirth O, Herzog GW, Hollerer I. 1982. ZnO dissolution kinetics by means of a ⁶⁵Zn tracer method. *Surf. Technol.* 15:43–52
- Galié S, García-Gutiérrez C, Miguélez EM, Villar CJ, Lombó F. 2018. Biofilms in the food industry: health aspects and control methods. *Front. Microbiol.* 9:898
- Ganjian M, Modaresifar K, Ligeon MRO, Kunkels LB, Tümer N, et al. 2019. Nature helps: toward bioinspired bactericidal nanopatterns. *Adv. Mater. Interfaces* 6(16):1900640
- Gleason KK. 2020. Chemically vapor deposited polymer nanolayers for rapid and controlled permeation of molecules and ions. *J. Vac. Sci. Technol. A* 38(2):020801
- Gleason KK. 2021. Controlled release utilizing initiated chemical vapor deposited (iCVD) of polymeric nanolayers. *Front. Bioeng. Biotechnol.* 9:632753
- Guo LJ. 2007. Nanoimprint lithography: methods and material requirements. *Adv. Mater.* 19(4):495–513
- Gupta M, Gleason KK. 2006. Large-scale initiated chemical vapor deposition of poly(glycidyl methacrylate) thin films. *Thin Solid Films* 515(4):1579–84
- Han S, Ji S, Abdullah A, Kim D, Lim H, Lee D. 2018. Applied surface science superhydrophilic nanopillar-structured quartz surfaces for the prevention of biofilm formation in optical devices. *Appl. Surf. Sci.* 429:244–52
- Harrand AS, Guariglia-Oropeza V, Skeens J, Kent D, Wiedmanna M. 2021. Nature versus nurture: assessing the impact of strain diversity and pre-growth conditions on *Salmonella enterica*, *Escherichia coli*, and *Listeria* species growth and survival on elected produce items. *Appl. Environ. Microbiol.* 87(6):e01925–20
- Harrand AS, Kovac J, Carroll LM, Guariglia-Oropeza V, Kent DJ, Wiedmann M. 2019. Assembly and characterization of a pathogen strain collection for produce safety applications: pre-growth conditions have a larger effect on peroxyacetic acid tolerance than strain diversity. *Front. Microbiol.* 10:1223
- Hasan J, Webb HK, Truong VK, Pogodin S, Baulin VA, et al. 2013. Selective bactericidal activity of nanopatterned superhydrophobic cicada *Psaltoda claripennis* wing surfaces. *Appl. Microbiol. Biotechnol.* 97(20):9257–62
- Hasan J, Xu Y, Yarlagaadda T, Schuetz M, Spann K, Yarlagaadda PKDV. 2020. Antiviral and antibacterial nanostructured surfaces with excellent mechanical properties for hospital applications. *ACS Biomater. Sci. Eng.* 6(6):3608–18
- Havelaar AH, Kirk MD, Torgerson PR, Gibb HJ, Hald T, et al. 2015. World Health Organization global estimates and regional comparisons of the burden of foodborne disease in 2010. *PLOS Med.* 12(12):e100193
- Hawi S, Goel S, Kumar V, Pearce O, Ayre WN, Ivanova EP. 2022. Critical review of nanopillar-based mechanobactericidal systems. *ACS Appl. Nano Mater.* 5(1):1–17
- Hayles A, Hasan J, Bright R, Palms D, Brown T, et al. 2021. Hydrothermally etched titanium: a review on a promising mechano-bactericidal surface for implant applications. *Mater. Today Chem.* 22:100622

- Hizal F, Zhuk I, Sukhishvili S, Busscher HJ, Van Der Mei HC, Choi CH. 2015. Impact of 3D hierarchical nanostructures on the antibacterial efficacy of a bacteria-triggered self-defensive antibiotic coating. *ACS Appl. Mater. Interfaces* 7(36):20304–13
- Ishak ML, Liu X, Jenkins J, Nobbs AH, Su B. 2020. Protruding nanostructured surfaces for antimicrobial and osteogenic titanium implants. *Coatings* 10(8):756
- Ivanova EP, Hasan J, Webb HK, Gervinskis G, Juodkazis S, et al. 2013. Bactericidal activity of black silicon. *Nat. Commun.* 4:2838
- Ivanova EP, Hasan J, Webb HK, Truong VK, Watson GS, et al. 2012. Natural bactericidal surfaces: mechanical rupture of *Pseudomonas aeruginosa* cells by cicada wings. *Small* 8(16):2489–94
- Ivanova EP, Linklater DP, Werner M, Baulin VA, Xu XM, et al. 2020. The multi-faceted mechano-bactericidal mechanism of nanostructured surfaces. *PNAS* 117(23):12598–605
- Jaggessar A, Shahali H, Mathew A, Yarlagadda PKDV. 2017. Bio-mimicking nano and micro-structured surface fabrication for antibacterial properties in medical implants. *J. Nanobiotechnol.* 15:64
- Jaggessar A, Yarlagadda PKDV. 2020. Modelling the growth of hydrothermally synthesised bactericidal nanostructures, as a function of processing conditions. *Mater. Sci. Eng. C* 108:110434
- Jang Y, Choi WT, Johnson CT, García AJ, Singh PM, et al. 2018. Inhibition of bacterial adhesion on nanotextured stainless steel 316L by electrochemical etching. *ACS Biomater. Sci. Eng.* 4(1):90–97
- Jenkins J, Mantell J, Neal C, Gholinia A, Verkade P, et al. 2020. Antibacterial effects of nanopillar surfaces are mediated by cell impedance, penetration and induction of oxidative stress. *Nat. Commun.* 11:1626
- Jiang R, Yi Y, Hao L, Chen Y, Tian L, et al. 2021. Thermoresponsive nanostructures: from mechano-bactericidal action to bacteria release. *ACS Appl. Mater. Interfaces* 13(51):60865–77
- Khlyustova A, Cheng Y, Yang R. 2020. Vapor-deposited functional polymer thin films in biological applications. *J. Mater. Chem. B* 8(31):6588–609
- Khlyustova A, Kirsch M, Ma X, Cheng Y, Yang R. 2022. Surfaces with antifouling-antimicrobial dual function via immobilization of lysozyme on zwitterionic polymer thin films. *J. Mater. Chem. B* 10(14):2728–39
- Kwiatkowski CF, Andrews DQ, Birnbaum LS, Bruton TA, Dewitt JC, et al. 2020. Scientific basis for managing PFAS as a chemical class. *Environ. Sci. Technol. Lett.* 7(8):532–43
- Lang J, Ma X, Chen P, Serota MD, Andre NM, et al. 2022. Haloperoxidase-mimicking CeO_{2-x} nanorods for the deactivation of human coronavirus OC43. *Nanoscale* 14(10):3731–37
- Leduc M, Kasra R, Van Heijenoort J. 1982. Induction and control of the autolytic system of *Escherichia coli*. *J. Bacteriol.* 152(1):26–34
- Li G, Tang L, Zhang X, Dong J. 2019. A review of factors affecting the efficiency of clean-in-place procedures in closed processing systems. *Energy* 178:57–71
- Linklater DP, Baulin VA, Juodkazis S, Crawford RJ, Stoodley P, Ivanova EP. 2020. Mechano-bactericidal actions of nanostructured surfaces. *Nat. Rev. Microbiol.* 19:9–12
- Linklater DP, De Volder M, Baulin VA, Werner M, Jessl S, et al. 2018. High aspect ratio nanostructures kill bacteria via storage and release of mechanical energy. *ACS Nano* 12(7):6657–67
- Linklater DP, Ivanova EP. 2022. Nanostructured antibacterial surfaces: What can be achieved? *Nano Today* 43:101404
- Linklater DP, Juodkazis S, Rubanov S, Ivanova EP. 2017. Comment on “Bactericidal effects of natural nanotopography of dragonfly wing on *Escherichia coli*.” *ACS Appl. Mater. Interfaces* 9(35):29387–93
- Linklater DP, Saita S, Murata T, Yanagishita T, Dekiwadia C, et al. 2022. Nanopillar polymer films as antibacterial packaging materials. *ACS Appl. Nano Mater.* 5(2):2578–91
- Liu CF, Lu YJ, Hu CC. 2018. Effects of anions and pH on the stability of ZnO nanorods for photoelectrochemical water splitting. *ACS Omega* 3(3):3429–39
- Liu L, Chen S, Xue Z, Zhang Z, Qiao X, et al. 2018. Bacterial capture efficiency in fluid bloodstream improved by bendable nanowires. *Nat. Commun.* 9:444
- Liu L, Chen S, Zhang X, Xue Z, Cui S, et al. 2020. Mechanical penetration of β -lactam-resistant Gram-negative bacteria by programmable nanowires. *Sci. Adv.* 6(27):eabb9593
- Liu T, Cui Q, Wu Q, Li X, Song K, et al. 2019. Mechanism study of bacteria killed on nanostructures. *J. Phys. Chem. B* 123(41):8686–96
- Liu Z, Yi Y, Song L, Chen Y, Tian L, et al. 2022. Biocompatible mechano-bactericidal nanopatterned surfaces with salt-responsive bacterial release. *Acta Biomater.* 141:198–208

- Machell J, Prior K, Allan R, Andresen JM. 2015. The water energy food nexus-challenges and emerging solutions. *Environ. Sci. Water Res. Technol.* 1(1):15–16
- Maleki E, Mirzaali MJ, Guagliano M, Bagherifard S. 2021. Analyzing the mechano-bactericidal effect of nano-patterned surfaces on different bacteria species. *Surf. Coat. Technol.* 408:126782
- Martin TP, Kooi SE, Chang SH, Sedransk KL, Gleason KK. 2007. Initiated chemical vapor deposition of antimicrobial polymer coatings. *Biomaterials* 28(6):909–15
- Maslar JE, Hurst WS, Bowers JJ, Hendricks JH. 2002. In situ raman spectroscopic investigation of stainless steel hydrothermal corrosion. *Corrosion* 58(9):739–47
- Masuda H, Asoh H, Watanabe M, Nishio K, Nakao M, Tamamura T. 2001. Square and triangular nanohole array architectures in anodic alumina. *Adv. Mater.* 13(3):189–92
- Mattila-Sandholm T, Wirtanen G. 1992. Biofilm formation in the industry: a review. *Food Rev. Int.* 8:573–603
- Mattsson K, Johnson EV, Malmendal A, Linse S, Hansson LA, Cedervall T. 2017. Brain damage and behavioural disorders in fish induced by plastic nanoparticles delivered through the food chain. *Sci. Rep.* 7:11452
- Mazinanian N, Odnevall Wallinder I, Hedberg Y. 2015. Comparison of the influence of citric acid and acetic acid as simulant for acidic food on the release of alloy constituents from stainless steel AISI 201. *J. Food Eng.* 145:51–63
- Meijer J, Du K, Gillner A, Hoffmann D, Kovalenko VS, et al. 2002. Laser machining by short and ultra-short pulses, state of the art and new opportunities in the age of the photons. *CIRP Ann. Manuf. Technol.* 51(2):531–50
- Michalska M, Divan R, Noirot P, Laible PD. 2021. Antimicrobial properties of nanostructured surfaces—demonstrating the need for a standard testing methodology. *Nanoscale* 13(41):17603–14
- Michalska M, Gambacorta F, Divan R, Aranson IS, Sokolov A, et al. 2018. Tuning antimicrobial properties of biomimetic nanopatterned surfaces. *Nanoscale* 10(14):6639–50
- Mimura S, Shimizu T, Shingubara S, Iwaki H, Ito T. 2022. Bactericidal effect of nanostructures: via lytic transglycosylases of *Escherichia coli*. *RSC Adv.* 12(3):1645–52
- Minoura K, Yamada M, Mizoguchi T, Kaneko T, Nishiyama K, et al. 2017. Antibacterial effects of the artificial surface of nanoimprinted moth-eye film. *PLOS ONE* 12(9):e0185366
- Mirzaali MJ, Van Dongen ICP, Tümer N, Weinans H, Yavari SA, Zadpoor AA. 2018. In-silico quest for bactericidal but non-cytotoxic nanopatterns. *Nanotechnology* 29(43):43LT02
- Modaresifar K, Azizian S, Ganjian M, Fratila-Apachitei LE, Zadpoor AA. 2019. Bactericidal effects of nanopatterns: a systematic review. *Acta Biomater.* 83:29–36
- Modaresifar K, Kunkels LB, Ganjian M, Tümer N, Hagen CW, et al. 2020. Deciphering the roles of inter-space and controlled disorder in the bactericidal properties of nanopatterns against *Staphylococcus aureus*. *Nanomaterials* 10(2):347
- Mousavi SM, Hashemi SA, Gholami A, Omidifar N, Zarei M, et al. 2021. Bioinorganic synthesis of polyrhodanine stabilized Fe₃O₄/graphene oxide in microbial supernatant media for anticancer and antibacterial applications. *Bioinorg. Chem. Appl.* 2021:9972664
- Negut I, Grumezescu V, Ficaï A, Grumezescu AM, Holban AM, et al. 2018. MAPLE deposition of *Nigella sativa* functionalized Fe₃O₄ nanoparticles for antimicrobial coatings. *Appl. Surf. Sci.* 455(1):513–21
- Nishiyama T, Hashimoto Y, Kusakabe H, Kumano T, Kobayashi M. 2014. Natural low-molecular mass organic compounds with oxidase activity as organocatalysts. *PNAS* 111(48):17152–57
- Nyankson E, Agbe H, Takyi GKS, Bensah YD, Sarkar DK. 2022. Recent advances in nanostructured superhydrophobic surfaces: fabrication and long-term durability challenges. *Curr. Opin. Chem. Eng.* 36:100790
- Park HH, Sun K, Lee D, Seong M, Cha C, Jeong HE. 2019a. Cellulose acetate nanoneedle array covered with phosphorylcholine moiety as a biocompatible and sustainable antifouling material. *Cellulose* 26(16):8775–88
- Park HH, Sun K, Seong M, Kang M, Park S, et al. 2019b. Lipid-hydrogel-nanostructure hybrids as robust biofilm-resistant polymeric materials. *ACS Macro Lett.* 8(1):64–69
- Paxson AT, Yagüe JL, Gleason KK, Varanasi KK. 2014. Stable dropwise condensation for enhancing heat transfer via the initiated chemical vapor deposition (iCVD) of grafted polymer films. *Adv. Mater.* 26(3):418–23

- Peter A, Lutey AHA, Faas S, Romoli L, Onuseit V, Graf T. 2020. Direct laser interference patterning of stainless steel by ultrashort pulses for antibacterial surfaces. *Opt. Laser Technol.* 123:105954
- Pham VTH, Truong VK, Mainwaring DE, Guo Y, Baulin VA, et al. 2014. Nanotopography as a trigger for the microscale, autogenous and passive lysis of erythrocytes. *J. Mater. Chem. B* 2(19):2819–26
- Piret JP, Vankoningsloo S, Mejia J, Noël F, Boilan E, et al. 2012. Differential toxicity of copper (II) oxide nanoparticles of similar hydrodynamic diameter on human differentiated intestinal Caco-2 cell monolayers is correlated in part to copper release and shape. *Nanotoxicology* 6(7):789–803
- Pogodin S, Hasan J, Baulin VA, Webb HK, Truong VK, et al. 2013. Biophysical model of bacterial cell interactions with nanopatterned cicada wing surfaces. *Biophys. J.* 104(4):835–40
- Reeja-Jayan B, Kovacic P, Yang R, Sojoudi H, Ugur A, et al. 2014. A route towards sustainability through engineered polymeric interfaces. *Adv. Mater. Interfaces* 1(4):1400117
- Robertson GL. 2013. *Food Packaging: Principles and Practice*. Boca Raton, FL: CRC Press. 3rd ed.
- Román-Kustas J, Hoffman JB, Reed JH, Gonsalves AE, Oh J, et al. 2020. Molecular and topographical organization: influence on cicada wing wettability and bactericidal properties. *Adv. Mater. Interfaces* 7(10):2000112
- Roy A, Chatterjee K. 2021. Theoretical and computational investigations into mechanobactericidal activity of nanostructures at the bacteria-biomaterial interface: a critical review. *Nanoscale* 13(2):647–58
- Scheldeman P, Herman L, Foster S, Heyndrickx M. 2006. *Bacillus sporothermodurans* and other highly heat-resistant spore formers in milk. *J. Appl. Microbiol.* 101(3):542–55
- Setlow P. 2007. I will survive: DNA protection in bacterial spores. *Trends Microbiol.* 15(4):172–80
- Sjollem J, Zaat SAJ, Fontaine V, Ramstedt M, Luginbuehl R, et al. 2018. In vitro methods for the evaluation of antimicrobial surface designs. *Acta Biomater.* 70:12–24
- Sukhanova A, Bozrova S, Sokolov P, Berestovoy M, Karaulov A, Nabiev I. 2018. Dependence of nanoparticle toxicity on their physical and chemical properties. *Nanoscale Res. Lett.* 13:44
- Sulka GD. 2008. Highly ordered anodic porous alumina formation by self-organized anodizing. In *Nanostructured Materials in Electrochemistry*, ed. A Eftekhari, pp. 1–116. Weinheim, Ger.: Wiley-VCH
- Sundara Selvam PS, Chinnadurai GS, Ganesan D, Kandan V. 2020. Eggshell membrane-mediated V₂O₅/ZnO nanocomposite: synthesis, characterization, antibacterial activity, minimum inhibitory concentration, and its mechanism. *Appl. Phys. A* 126:893
- Takei S, Hanabata M. 2015. Ultraviolet nanoimprint lithography using cyclodextrin-based porous template for pattern failure reduction. *Appl. Phys. Lett.* 107:141904
- Takei S, Yasuda K. 2020. Fabrication of nanostructured antibacterial film derived from oligoglucosamine in ultraviolet nanoimprint lithography using a solvent-permeable template. *Appl. Phys. Express* 13:106506
- Talbert JN, Goddard JM. 2013. Influence of nanoparticle diameter on conjugated enzyme activity. *Food Bioprod. Process.* 91(4):693–99
- Tan R, Marzolini N, Jiang P, Jang Y. 2020. Bio-inspired polymer thin films with non-close-packed nanopillars for enhanced bactericidal and antireflective properties. *ACS Appl. Polym. Mater.* 2(12):5808–16
- Thimothe J, Nightingale KK, Gall K, Scott VN, Wiedmann M. 2004. Tracking of *Listeria monocytogenes* in smoked fish processing plants. *J. Food Prot.* 67(2):328–41
- Tiller JC, Liao CJ, Lewis K, Klivanov AM. 2001. Designing surfaces that kill bacteria on contact. *PNAS* 98(11):5981–85
- Toole GO, Kaplan HB, Kolter R. 2000. Biofilm formation as microbial development. *Annu. Rev. Microbiol.* 54:49–79
- Tripathy A, Sen P, Su B, Briscoe WH. 2017. Natural and bioinspired nanostructured bactericidal surfaces. *Adv. Colloid Interface Sci.* 248:85–104
- Tu Y, Lv M, Xiu P, Huynh T, Zhang M, et al. 2013. Destructive extraction of phospholipids from *Escherichia coli* membranes by graphene nanosheets. *Nat. Nanotechnol.* 8:594–601
- Unger K, Salzmann P, Masciullo C, Cecchini M, Koller G, Coclite AM. 2017. Novel light-responsive biocompatible hydrogels produced by initiated chemical vapor deposition. *ACS Appl. Mater. Interfaces* 9(20):17408–16
- Valiei A, Lin N, Bryce JF, McKay G, Canva M, et al. 2020. Hydrophilic mechano-bactericidal nanopillars require external forces to rapidly kill bacteria. *Nano Lett.* 20(8):5720–27

- Velic A, Hasan J, Li Z, Yarlagadda PKDV. 2021. Mechanics of bacterial interaction and death on nanopatterned surfaces. *Biophys. J.* 120(2):217–31
- Vorst KL, Todd ECD, Ryser ET. 2006. Transfer of *Listeria monocytogenes* during slicing of turkey breast, bologna, and salami with simulated kitchen knives. *J. Food Prot.* 69(12):2939–46
- Wagner S, Reemtsma T. 2019. Things we know and don't know about nanoplastic in the environment. *Nat. Nanotechnol.* 14(4):300–1
- Wandiyanto JV, Tamanna T, Linklater DP, Truong VK, Al Kobaisi M, et al. 2020. Tunable morphological changes of asymmetric titanium nanosheets with bactericidal properties. *J. Colloid Interface Sci.* 560:572–80
- Watson GS, Green DW, Schwarzkopf L, Li X, Cribb BW, et al. 2015. A gecko skin micro/nano structure: a low adhesion, superhydrophobic, anti-wetting, self-cleaning, biocompatible, antibacterial surface. *Acta Biomater.* 21:109–22
- Watson GS, Green DW, Watson JA, Zhou Z, Li X, et al. 2019. A simple model for binding and rupture of bacterial cells on nanopillar surfaces. *Adv. Mater: Interfaces* 6(10):1801646
- Worgull M, Schneider M, Röhrig M, Meier T, Heilig M, et al. 2013. Hot embossing and thermoforming of biodegradable three-dimensional wood structures. *RSC Adv.* 3(43):20060–64
- Wu B, Zhou M, Li J, Ye X, Li G, Cai L. 2009. Superhydrophobic surfaces fabricated by microstructuring of stainless steel using a femtosecond laser. *Appl. Surf. Sci.* 256(1):61–66
- Wu S, Zuber F, Maniura-Weber K, Brugger J, Ren Q. 2018. Nanostructured surface topographies have an effect on bactericidal activity. *J. Nanobiotechnol.* 16:20
- Xie Y, Qu X, Li J, Li D, Wei W, et al. 2020. Ultrafast physical bacterial inactivation and photocatalytic self-cleaning of ZnO nanoarrays for rapid and sustainable bactericidal applications. *Sci. Total Environ.* 738:139714
- Yamada M, Minoura K, Mizoguchi T, Nakamatsu K, Taguchi T, et al. 2018. Antibacterial effects of nano-imprinted motheye film in practical settings. *PLOS ONE* 13(10):e0198300
- Yang R, Asatekin A, Gleason KK. 2012. Design of conformal, substrate-independent surface modification for controlled protein adsorption by chemical vapor deposition (CVD). *Soft Matter* 8(1):31–43
- Yi Y, Jiang R, Liu Z, Dou H, Song L, et al. 2022. Bioinspired nanopillar surface for switchable mechano-bactericidal and releasing actions. *J. Hazard. Mater.* 432:128658
- Yu H, Zhang Z, Han M, Hao X, Zhu F. 2005. A general low-temperature route for large-scale fabrication of highly oriented ZnO nanorod/nanotube arrays. *J. Am. Chem. Soc.* 127(8):2378–79
- Yuan Y, Zhang Y. 2017. Enhanced biomimic bactericidal surfaces by coating with positively-charged ZIF nano-dagger arrays. *Nanomed. Nanotechnol. Biol. Med.* 13(7):2199–207
- Zhao S, Li Z, Linklater DP, Han L, Jin P, et al. 2022. Programmed death of injured *Pseudomonas aeruginosa* on mechano-bactericidal surfaces. *Nano Lett.* 22(3):1129–37